

AFML-TR-75-121

F13EC

#12

FBE

AD-A018670

# TWO DIMENSIONAL STRESS INTENSITY FACTOR SOLUTIONS FOR RADIALY CRACKED RINGS

*METALS BEHAVIOR BRANCH  
METALS AND CERAMICS DIVISION*

OCTOBER 1975

TECHNICAL REPORT AFML-TR-75-121  
FINAL REPORT FOR PERIOD MARCH 1974 - DECEMBER 1974.

Approved for public release; distribution unlimited

AIR FORCE MATERIALS LABORATORY  
AIR FORCE WRIGHT AERONAUTICAL LABORATORIES  
Air Force Systems Command  
Wright-Patterson Air Force Base, Ohio 45433

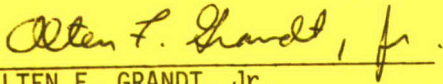
20071128027

NOTICE

When Government drawings, specifications, or other data are used for any purpose other than in connection with a definitely related Government procurement operation, the United States Government thereby incurs no responsibility nor any obligation whatsoever; and the fact that the government may have formulated, furnished, or in any way supplied the said drawings, specifications, or other data, is not to be regarded by implication or otherwise as in any manner licensing the holder or any other person or corporation, or conveying any rights or permission to manufacture, use, or sell any patented invention that may in any way be related thereto.

This report has been reviewed and cleared for open publication and/or public release by the Office of Information (OI) in accordance with AFR 190-17 and DOD 5230.9. There is no objection to unlimited distribution of this report to the public at large, or by DDC to the National Technical Information Service (NTIS).

This technical report has been reviewed and is approved for publication.



ALTEN F. GRANDT, Jr.  
Project Engineer

FOR THE COMMANDER



VINCENT J. RUSSO  
Chief, Metals Behavior Branch  
Metals and Ceramics Division

*Copies of this report should not be returned unless return is required by security considerations, contractual obligations, or notice on a specific document.*

UNCLASSIFIED

SECURITY CLASSIFICATION OF THIS PAGE (When Data Entered)

REPORT DOCUMENTATION PAGE		READ INSTRUCTIONS BEFORE COMPLETING FORM
1. REPORT NUMBER <b>AFML-TR-75-121</b>	2. GOVT ACCESSION NO.	3. RECIPIENT'S CATALOG NUMBER
4. TITLE (and Subtitle) <b>TWO DIMENSIONAL STRESS INTENSITY FACTOR SOLUTIONS FOR RADIALLY CRACKED RINGS</b>		5. TYPE OF REPORT & PERIOD COVERED <b>Final Report March 74 - December 74</b>
7. AUTHOR(s) <b>Alten F. Grandt, Jr.</b>		6. PERFORMING ORG. REPORT NUMBER
9. PERFORMING ORGANIZATION NAME AND ADDRESS <b>Air Force Materials Laboratory Air Force Systems Command Wright-Patterson Air Force Base, OH 45433</b>		8. CONTRACT OR GRANT NUMBER(s)
11. CONTROLLING OFFICE NAME AND ADDRESS <b>Same</b>		10. PROGRAM ELEMENT, PROJECT, TASK AREA & WORK UNIT NUMBERS <b>7351-06A4</b>
14. MONITORING AGENCY NAME & ADDRESS (if different from Controlling Office)		12. REPORT DATE <b>October 1975</b>
		13. NUMBER OF PAGES <b>26</b>
		15. SECURITY CLASS. (of this report) <b>Unclassified</b>
		15a. DECLASSIFICATION/DOWNGRADING SCHEDULE
16. DISTRIBUTION STATEMENT (of this Report) <b>Approved for public release; distribution unlimited.</b>		
17. DISTRIBUTION STATEMENT (of the abstract entered in Block 20, if different from Report)		
18. SUPPLEMENTARY NOTES		
19. KEY WORDS (Continue on reverse side if necessary and identify by block number) <b>stress intensity factors fracture mechanics linear superposition weight functions</b>		
20. ABSTRACT (Continue on reverse side if necessary and identify by block number) <b>A weight function technique is used to obtain mode I stress intensity factor solutions for radially cracked rings loaded with arbitrary crack face pressure. When the crack face pressure is defined as the hoop stress occurring in an unflawed member subjected to complex loading, stress intensity factor calibrations may be obtained by the linear superposition method. This procedure is demonstrated with calculations for rings loaded in compression, for cylinders under internal and external pressure, and for centrifugal stresses induced by</b> <b>(abstract cont)</b>		

DD FORM 1473

1 JAN 73

EDITION OF 1 NOV 65 IS OBSOLETE

UNCLASSIFIED

SECURITY CLASSIFICATION OF THIS PAGE (When Data Entered)

UNCLASSIFIED

SECURITY CLASSIFICATION OF THIS PAGE(When Data Entered)

abstract continued:

rotating the rings. Solutions obtained in this manner agree well with previous results found by other methods. It is suggested that the solution and techniques described here may have further application to other practical problems.

UNCLASSIFIED

SECURITY CLASSIFICATION OF THIS PAGE(When Data Entered)

FOREWORD

This report was prepared by the Metals Behavior Branch, Metals and Ceramics Division, Air Force Materials Laboratory. The work was performed inhouse under Project 7351, "Metallic Materials For Air Force Weapon System Components," Task 735106, "Behavior of Metals Used in Flight Vehicle and Engine Structural Applications," and was administered under the direction of the Air Force Materials Laboratory, Air Force Systems Command, Wright-Patterson Air Force Base, Ohio. The research was conducted by Alten F. Grandt, Jr. of the Metals Behavior Branch.

The report covers work conducted March 1974 through December 1974 and was submitted in May 1975.

The author is grateful to A.T. Jones for providing the original stress intensity factor and COD curves of Reference 10 needed to construct the weight functions employed here. The assistance of C.W. Smith in pointing out a numerical error in one of the examples in an earlier draft is also appreciated.

TABLE OF CONTENTS

SECTION		PAGE
I	INTRODUCTION	1
II	DEVELOPMENT OF CRACK FACE PRESSURE SOLUTION	2
III	LINEAR SUPERPOSITION APPLICATIONS	6
	1. Compressive Loading	6
	2. Remote Tension	7
	3. Pressurized Cylinders	8
	4. Centrifugal Loading	8
	5. Notched Turbine Disk	9
	6. Thermally Stressed Disks	10
IV	CONCLUDING REMARKS	11
	REFERENCES	22

## LIST OF ILLUSTRATIONS

FIGURE		PAGE
1	Radially Cracked Ring Loaded with Crack Face Pressure (Case 2)	13
2	Radially Cracked Ring Loaded in Compression (Case 1)	14
3	Stress Intensity Factor Calibration for a Cracked Ring Loaded in Compression ( $R_i/R_o = 0.5$ )	15
4	Stress Intensity Factor Calibration for a Cracked Ring Loaded in Remote Tension ( $R_i/R_o = 0.5$ )	16
5	Stress Intensity Factor Calibration for a Cracked Ring Loaded in Remote Tension ( $R_i/R_o = 0.8$ )	17
6	Stress Intensity Factor Calibration for a Cracked Cylinder Under Internal Pressure ( $R_i/R_o = 0.5$ )	18
7	Stress intensity Factor Calibration for a Cracked Cylinder Under Internal Pressure ( $R_i/R_o = 0.8$ )	19
8	Stress Intensity Factor Calibration for a Cracked Ring Rotating With Angular Velocity $\omega$	20
9	Stress Intensity Factor Calibration for a Crack Emanating from a Keyway in a Spinning Turbine Disk	21
10	Stress Intensity Factor Calibration for a Cracked Ring Subjected to a Thermal Gradient	22

SECTION I  
INTRODUCTION

A stress intensity factor ( $K_I$ ) solution was obtained in previous work [1] for radially cracked holes in large plates loaded with arbitrary crack face pressure. When the pressure is specified as the hoop stress surrounding an unflawed fastener hole subjected to complex loading, stress intensity factors are readily found for cracked members by the linear superposition method [1-5]. Stress intensity factor calibrations obtained in this manner agreed well with results found by independent analytical [6] and experimental [7] methods.

A similar procedure is employed in this paper to obtain  $K_I$  calibrations for two-dimensional rings containing one and two radial cracks. This configuration might be used to model service cracks found in thick walled cylinders, turbine disks, or as free boundary corrections for the fastener hole cracks discussed in Reference 1.

First, a weight function technique is used to find  $K_I$  for the crack face pressure loading shown in Figure 1. Next, the linear superposition method is employed to obtain stress intensity factor calibrations for flawed rings in compression, for cylinders under internal and external pressure, for rotating rings, and for thermally loaded cylinders. Plane strain results are given for members with inner to outer wall radius ratios ( $R_i/R_o$ ) of 0.5 and 0.8. Crack lengths varied up to 0.9 of the wall thickness under mode I loading.

## SECTION II

## DEVELOPMENT OF CRACK FACE PRESSURE SOLUTION

Rice [8] has shown that knowledge of the stress intensity factor and displacement field for a given flaw geometry and loading (case 1) enable construction of a weight function which depends only on geometry. With the weight function one may then obtain  $K_I$  for any other symmetric loading (case 2) applied to the same geometry. This procedure is similar to weight function techniques used earlier by Bueckner [5] for edge cracked strips, and has recently been applied to other problems of engineering interest in References 1 and 9.

The problem solved in the present work consists of the radially cracked ring (and its doubly cracked symmetric counterpart) shown in Figure 1. Here  $R_i$  and  $R_o$  are the inner and outer radii of the ring,  $a$  is the crack length, and  $p(x)$  is an arbitrary pressure loading perpendicular to the crack faces. The pressure distribution is symmetric with respect to the  $x$ -axis and does not allow the crack surfaces to close in compression.

The known (case 1) problem used to construct the weight function is shown in Figure 2. Although the geometry is identical to Figure 1, the loading differs in that a concentrated compressive force  $P$  is applied along the crack axis. Jones [10] has reported finite element solutions to the stress intensity factor and crack mouth displacement ( $\eta_o$ ) for ring shapes of  $R_i/R_o = 0.5, 0.8, 0.9, \text{ and } 0.945$ . This information is

used here to construct the weight function required to solve the crack face pressure loading for 0.5 and 0.8  $R_i/R_0$  aspect ratios.

Following Rice [8], the desired stress intensity factor is given by

$$K_I = \int_{\Gamma} \underline{s} \cdot \underline{h} \, d\Gamma + \int_A \underline{f} \cdot \underline{h} \, dA \quad (1)$$

Here  $\underline{s}$  is the stress vector acting on boundary  $\Gamma$  chosen around the crack tip, while  $\underline{f}$  is the body force in region A defined by  $\Gamma$ . The vector  $\underline{h}$  is the weight function determined for the flaw geometry by the case 1 loading. This weight function is given by

$$\underline{h} = \underline{h}(x,y,a) = \frac{H}{2K} \frac{\partial \underline{u}}{\partial a} \quad (2)$$

Here K is the case 1 stress intensity factor and  $\underline{u}$  is the corresponding displacement field. For plane strain conditions, H is the constant  $E/(1-\nu^2)$ , where E is the elastic modulus and  $\nu$  is Poisson's ratio.

Defining the case 1 loading as the compressive force P shown in Figure 2, and choosing the boundary  $\Gamma$  to consist of the inner ring perimeter and the crack faces as shown in Figure 1, specific terms in Equation 1 become

$$\tilde{s} = \begin{cases} s_x = 0 \\ s_y = p(x) \end{cases} \quad \text{along the crack faces} \quad (3)$$

$$s_x = s_y = 0 \quad \text{along the inner ring boundary}$$

$$\tilde{f} = 0 \quad (\text{no body forces in area A}) \quad (4)$$

and

$$h_y = \frac{H}{2K_J} \frac{\partial \eta}{\partial a} \quad \text{along the crack faces} \quad (5)$$

Here  $K_J$  is Jones' stress intensity factor solution and  $\eta$  is the y-component of the crack surface displacement ( $u_y$ ). Now, combining Equations 1-5 yields the desired  $K_I$  solution.

$$K_I = \frac{H}{K_J} \int_0^a P(x) \frac{\partial \eta}{\partial a} dx \quad (6)$$

Since the pressure  $p(x)$  will be given by the specific problem of interest, the only undefined term in Equation 6 is the partial derivative  $\frac{\partial \eta}{\partial a}$ . Although only the crack mouth displacement  $\eta_0$  (the value of  $\eta$  at  $x = 0$ ) is given by Jones [10], it is shown in Reference 1 that the entire crack shape (i.e.  $\eta$  for  $0 \leq x \leq a$ ) can be constructed to satisfactory accuracy from knowledge of  $\eta_0$  and  $K_I$ . This procedure involves using a conic section given by Orange [11] for fitting edge crack surface displacements. As shown in Reference 1, crack shapes determined by

the conic section for radially flawed holes loaded in remote tension agree well with crack surface displacements found by the finite element method. Thus, differentiating the conic section representation for  $\eta$ , Equation 6 is readily solved for  $K_I$ . Applications of this solution by means of the linear superposition method are presented in the following section.

### SECTION III

#### LINEAR SUPERPOSITION APPLICATIONS

Through the linear superposition principle, the solution to the problem shown in Figure 1 may be used to convert stress data for unflawed rings and cylinders into stress intensity factors for cracked members. This conversion is accomplished by defining the pressure  $p(x)$  in Equation 6 as the unflawed hoop stress occurring along a radial line coinciding with the desired path of crack propagation. It has been shown previously [1,3,5,7] that stress intensity factors found by the linear superposition method correspond to values determined directly for cracked components. The application of the solution derived in the previous section is demonstrated below with examples of calculations for flawed rings and cylinders. These examples have been chosen to demonstrate that the weight function/linear superposition method gives results of acceptable accuracy and may be applied to complex engineering problems with relative ease.

#### 1. COMPRESSIVE LOADING

The compressively loaded ring shown in Figure 2 provides a convenient check on the accuracy of the present solution. The stress distribution for an unflawed ring of aspect ratio  $R_i/R_o = 0.5$  subjected to a compressive force is given in Reference 12. By defining  $p(x)$  as a least squares polynomial representation for the hoop stress perpendicular to the loading axis, Equation 6 gives the stress intensity factor calibrations for single and double cracked rings shown in Figure 3.

Note that although the linear superposition values slightly exceed Jones' finite element analysis, with the exception of long double cracks ( $a/(R_0-R_i) \geq 0.75$ ), both methods agree within five percent. In addition, experimental measurements by the compliance derivative method reported by Jones [10] for 7075 T6 aluminum cylinders agree well with the single crack superposition results.

The numerical approximations employed in the present calculations most likely explain the differences indicated in Figure 3. Since only the crack mouth displacement data were reported by Jones, it was necessary, for example, to approximate the remaining crack shape with a conic section as described previously. Other sources of error lie in the least squares representation for  $p(x)$  and in the numerical integration of Equation 6. In spite of these approximations, however, the accuracy of the linear superposition solution is adequate for most engineering calculations.

## 2. REMOTE TENSION

Flawed rings loaded in remote tension as shown in Figures 4 and 5 provide another test problem for the present analysis. Bowie and Freese [13] have obtained stress intensity factor solutions by conformal mapping techniques for several single crack ring geometries. Unflawed stresses for aspect ratios of 0.5 and 0.8 were taken from the remote tension analysis reported in Reference 14 and used to define  $p(x)$  as before. Linear superposition results computed from Equation 6 are compared with Bowie and Freese's data in Figures 4 and 5. The dashed lines in Figure 5 represent single crack values of questionable accuracy

as reported by Bowie and Freese. Note again the good agreement between single crack results computed by the simple linear superposition method and those obtained by more sophisticated means. Since Bowie and Freese did not report solutions for double cracks, the linear superposition values shown for two cracks in Figures 4 and 5 represent new calibrations.

### 3. PRESSURIZED CYLINDERS

Cylinders loaded with an internal pressure  $P$  as shown in Figures 6 and 7 were considered by the present method. The unflawed hoop stress analysis for internal bore pressure reported in Reference 14 was used to define  $p(x)$  in Equation 6. The single and double flaw results are shown in Figures 6 and 7 for aspect ratios of 0.5 and 0.8. Since the crack faces of the cylinder will also be subjected to the pressure  $p$ , results due to constant crack face loading are also shown. The complete solution obtained by adding the bore pressure and crack face pressure results is equivalent to the remote tension results of Figures 4 and 5. Note that as the ring becomes thinner ( $R_1/R_0$  gets larger), the effect of the crack face loading decreases with respect to the bore pressure. This trend was continued with other unreported results for  $R_1/R_0 = 0.9$  rings.

### 4. CENTRIFUGAL LOADINGS

The present solution may also be used to study cracks which may occur in members used to approximate rotating turbine disks. Consider, for example, the centrifugal loading caused by rotating a ring of density  $\rho$  with an angular velocity  $\omega$  as shown in Figure 8. The unflawed hoop stresses for rotating rings are reported in Reference 12. Fitting this

analysis with a polynomial for  $p(x)$  as before, Equation 6 gives the single and double crack stress intensity factors in Figure 8. Previous estimates for the single flaw case are reported by Williams and Isherwood in Reference 15. Their results, obtained by an approximate method based on the mean stress in the unflawed member, are seen to agree closely with the present analysis.

#### 5. NOTCHED TURBINE DISK

The engineering utility of the present solution may be further demonstrated with a more complex example. Owen and Griffiths [16] have reported a finite element analysis for radial cracks occurring at the keyway in a rotating steam turbine disk. Their idealized two-dimensional model for the actual disk is shown in Figure 9 and is described in more detail in Reference 16. The cracks occur at the root of a 1-inch deep keyway in the uniform thickness ring with  $R_i = 9$  inch and  $R_o = 16$  inches. Stress intensity factors found by the compliance derivative method by Owen and Griffiths are shown in Figure 9. The results given are for a disk with the material properties shown in Figure 9 rotating with an angular velocity  $\omega = 3000$  rpm and with a uniform blade force  $F$  of 7400 psi acting on the circumference of the rim.

The unflawed hoop stress distribution at the notch is also reported for these operating conditions in Reference 16. Defining  $p(x)$  as the polynomial representation for stresses with and without the blade forces, Equation 6 gives the single crack results shown in Figure 9. Note that the linear superposition values agree well with the finite element analysis for small crack lengths, but exceed Owen and Griffiths' data by as much as fifteen percent for the longer flaws. This latter

difference may be due to the fact that it was necessary here to approximate the actual  $R_i/R_o = 9/16 = 0.56$  disk with a ring shape of  $R_i/R_o = 0.5$ . This approximation could, of course, be eliminated if the  $K_I$  and displacement data were available to construct the actual weight function for a 0.56 aspect ratio disk. In addition, the effect of the notch was ignored in the calculations of Equation 6 by assuming the x-coordinate originated at the tip of the keyway. The influence of the keyway is, however, represented in the unflawed hoop stress  $p(x)$ .

## 6. THERMALLY STRESSED DISKS

Consider a  $R_i/R_o = 0.5$  ring to be subjected to a thermal gradient  $\Delta T = T_o - T_i$  as shown in Figure 10. The thermal stress field for an unflawed disk is given in Reference 12 as a function of  $\Delta T$ , the coefficient of thermal expansion  $\alpha$ , the elastic modulus  $E$ , and Poisson's Ratio  $\nu$ . Defining  $p(x)$  in Equation 6 as the uncracked stress distribution for  $T_o > T_i$ , and assuming  $\nu = 0.3$ , gives the stress intensity factor results in Figure 10. Examining the absolute value of  $K_I$ , rather than the dimensionless coefficient  $K_I/[\alpha E(T_o - T_i)\sqrt{\pi a}]$  plotted in Figure 10, it is seen that  $K_I$  peaks at  $a/(R_o - R_i) = 0.65$  for the double crack problem and at  $a/(R_o - R_i) = 0.35$  for a single flaw. This decreasing  $K_I$  result is in qualitative agreement with experiments in thermally stressed graphite rings which indicate that radial cracks may initially extend and then arrest under certain temperature conditions (17).

A stress intensity factor solution has been described for radially cracked rings loaded with arbitrary crack face pressure. The method of solution employs a weight function technique which allows the use of existing stress intensity factor and crack displacement data for a given loading to calculate  $K_I$  for other loadings applied to the same geometry. The crack face pressure solution obtained in this manner is then taken in conjunction with the linear superposition method to solve several flawed ring problems. In applying the linear superposition method, the arbitrary crack face pressure is simply defined as the unflawed hoop stress occurring in the radial crack growth direction of interest. Stress intensity factors calculated from the crack face pressure solution through the linear superposition method agree well with previous solutions obtained by more complex experimental and analytical techniques.

The ability to convert unflawed hoop stress data into accurate  $K_I$  solutions for cracked members has significant engineering implications. Since stress intensity factors are readily obtained from the uncracked results, computation time and costs are greatly reduced. If unflawed hoop stress solutions are available for the uncracked component, as was the case for the examples discussed here, stress intensity results are obtained immediately through the solution of Equation 6. If, on the other hand, uncracked stresses are unavailable, it is much quicker and easier to obtain the unflawed solution required for the linear superposition method and then solve Equation 6, than to analyze the singular

crack tip stress field directly. Furthermore, only one unflawed stress distribution is required to calculate  $K_I$  for a wide range of crack lengths, while methods which consider the crack tip directly must be resolved for each crack length to obtain the complete calibration curve.

As fracture mechanics criteria continue to be included in future design criteria (see Reference 18, for example), there will be an increasing need for the engineer to quickly find stress intensity factors for a variety of component shapes and loadings. The weight function/linear superposition method discussed here for flawed rings, and in Reference 1 for cracked fastener holes, provides the engineer with an efficient tool for making the necessary  $K_I$  calculations. Since the proposed method still requires accurate  $K_I$  and crack displacement data for one loading configuration to compute the weight function, other sophisticated analysis methods (e.g., finite elements, conformal mapping, etc.) are still needed for different geometries. Once the initial problem is solved, however, the present technique may then be used to rapidly find calibrations for many other loading configurations.

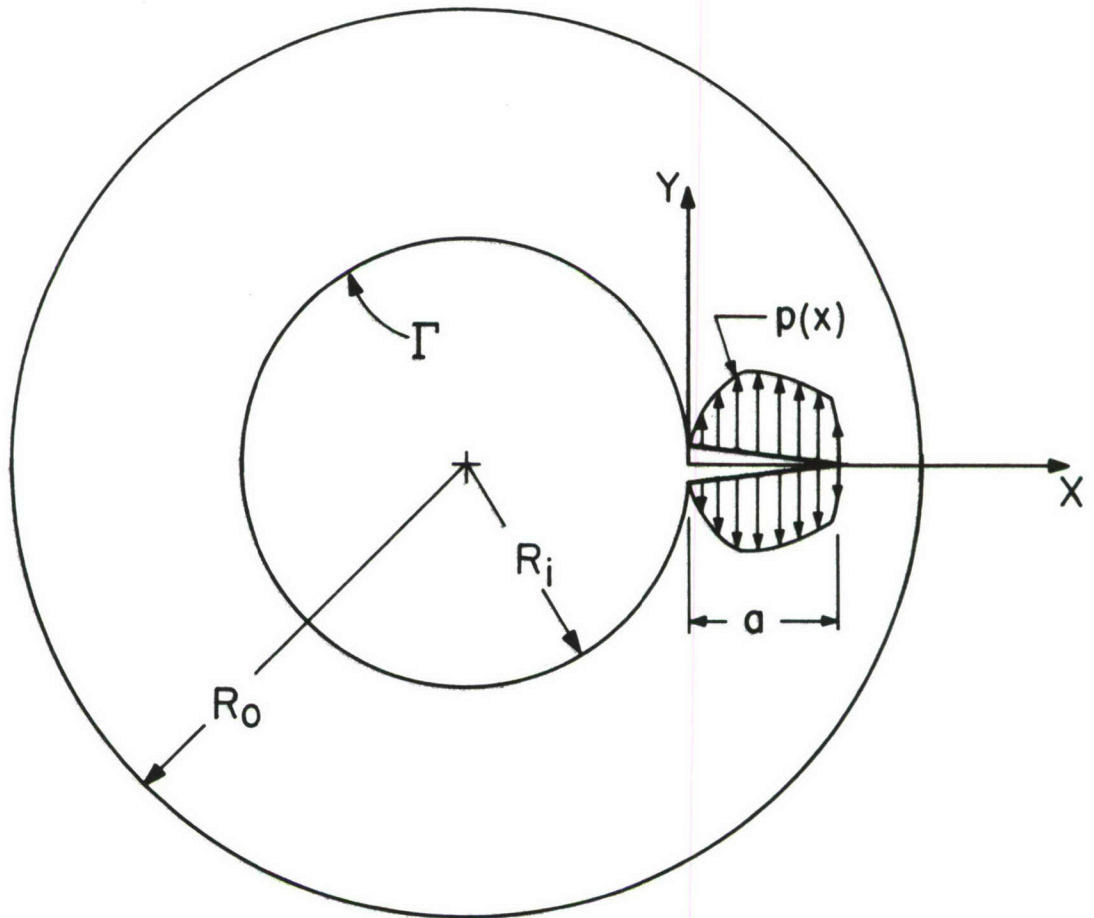


Figure 1. Radially Cracked Ring Loaded with Crack Face Pressure (Case 2)

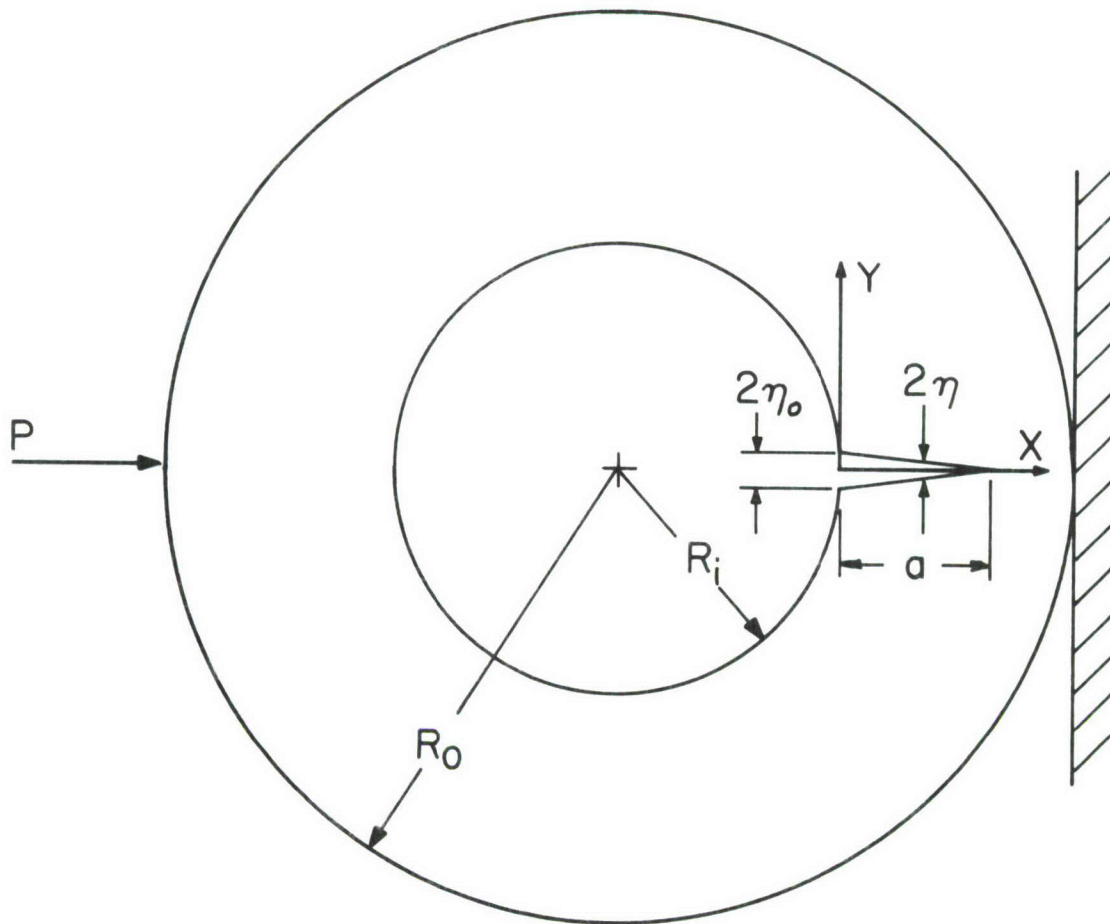


Figure 2. Radially Cracked Ring Loaded in Compression (Case 1)

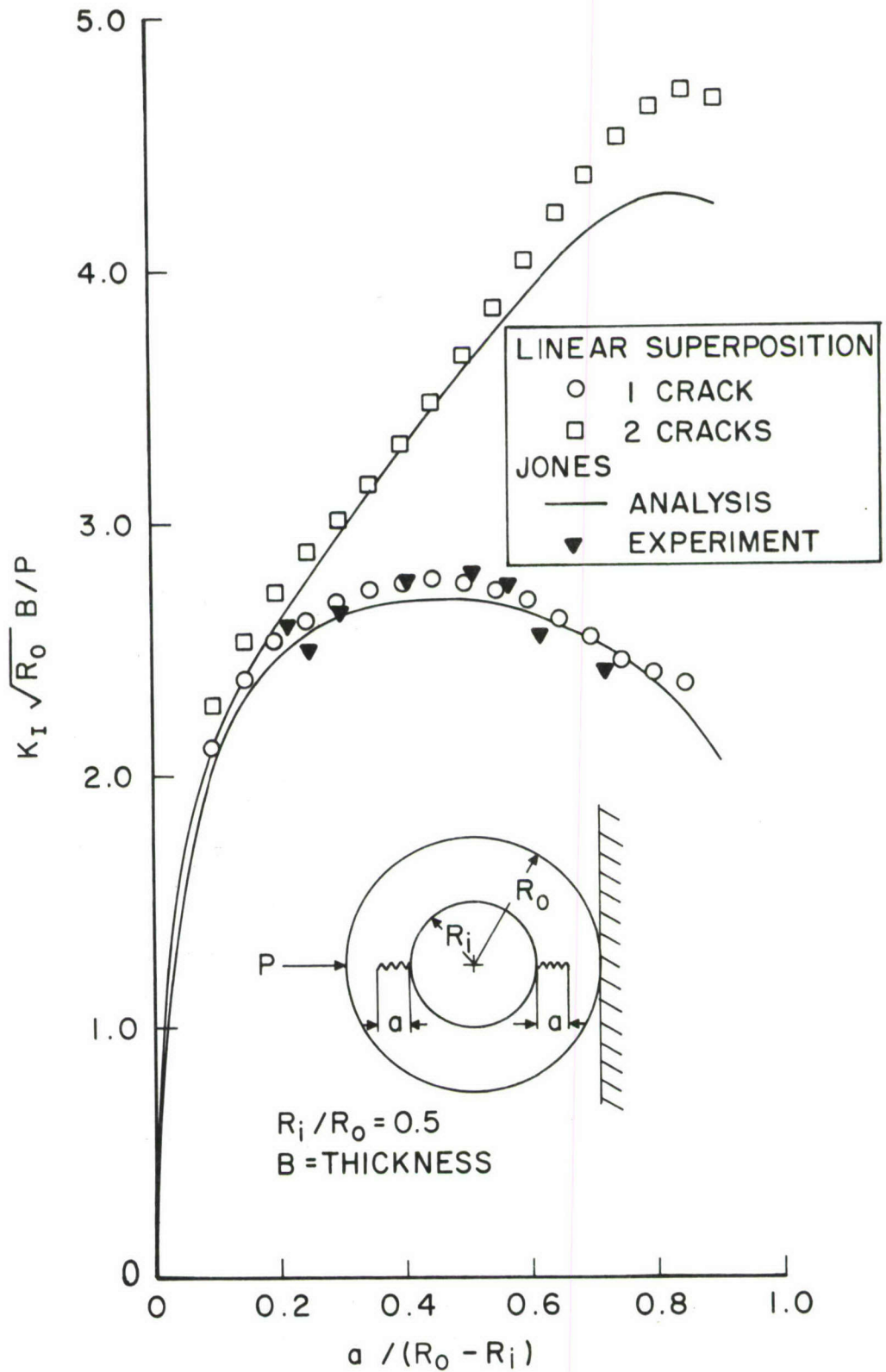


Figure 3. Stress Intensity Factor Calibration for a Cracked Ring Loaded in Compression ( $R_i/R_0 = 0.5$ )

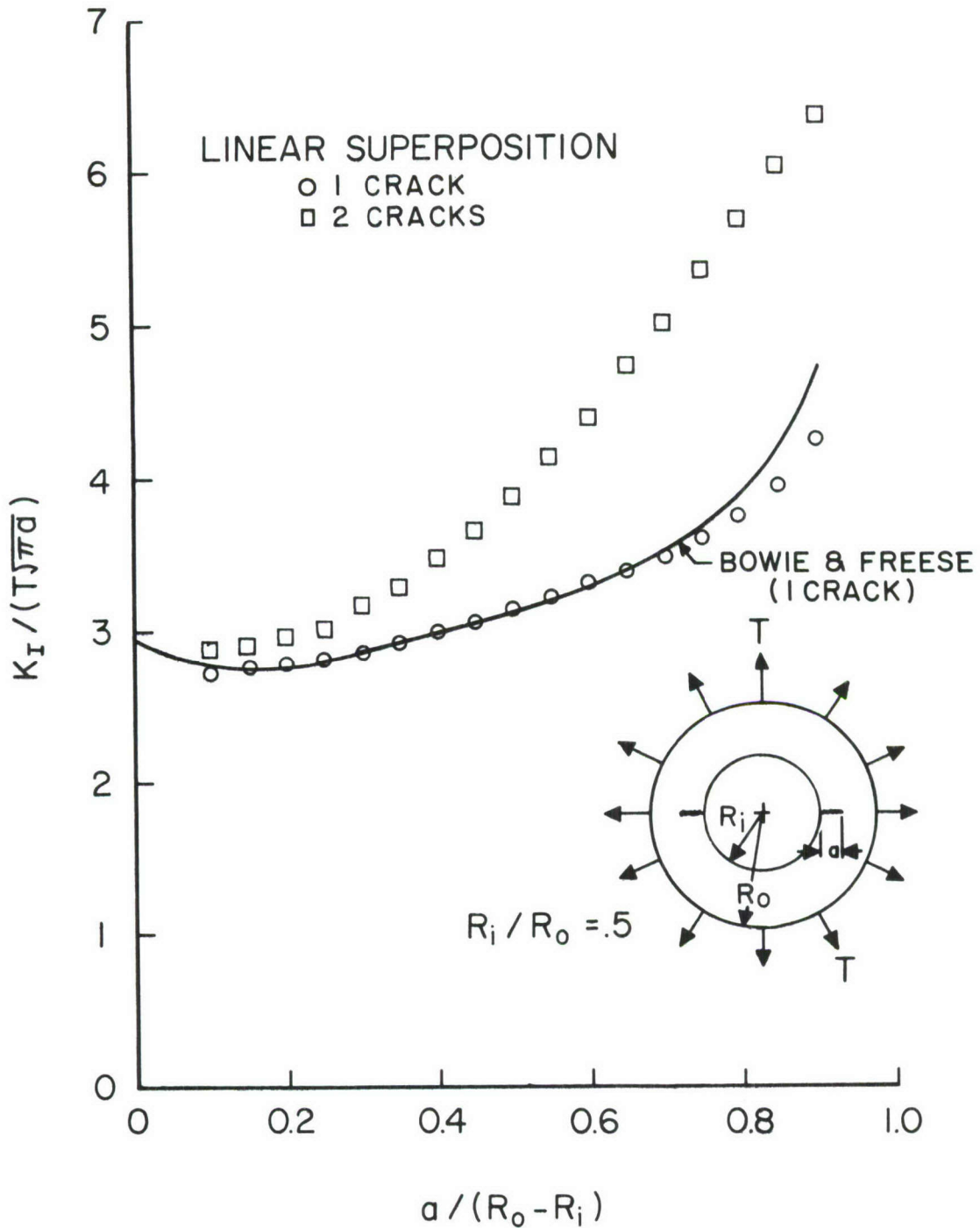


Figure 4. Stress Intensity Factor Calibration for a Cracked Ring Loaded in Remote Tension ( $R_i/R_o = 0.5$ )

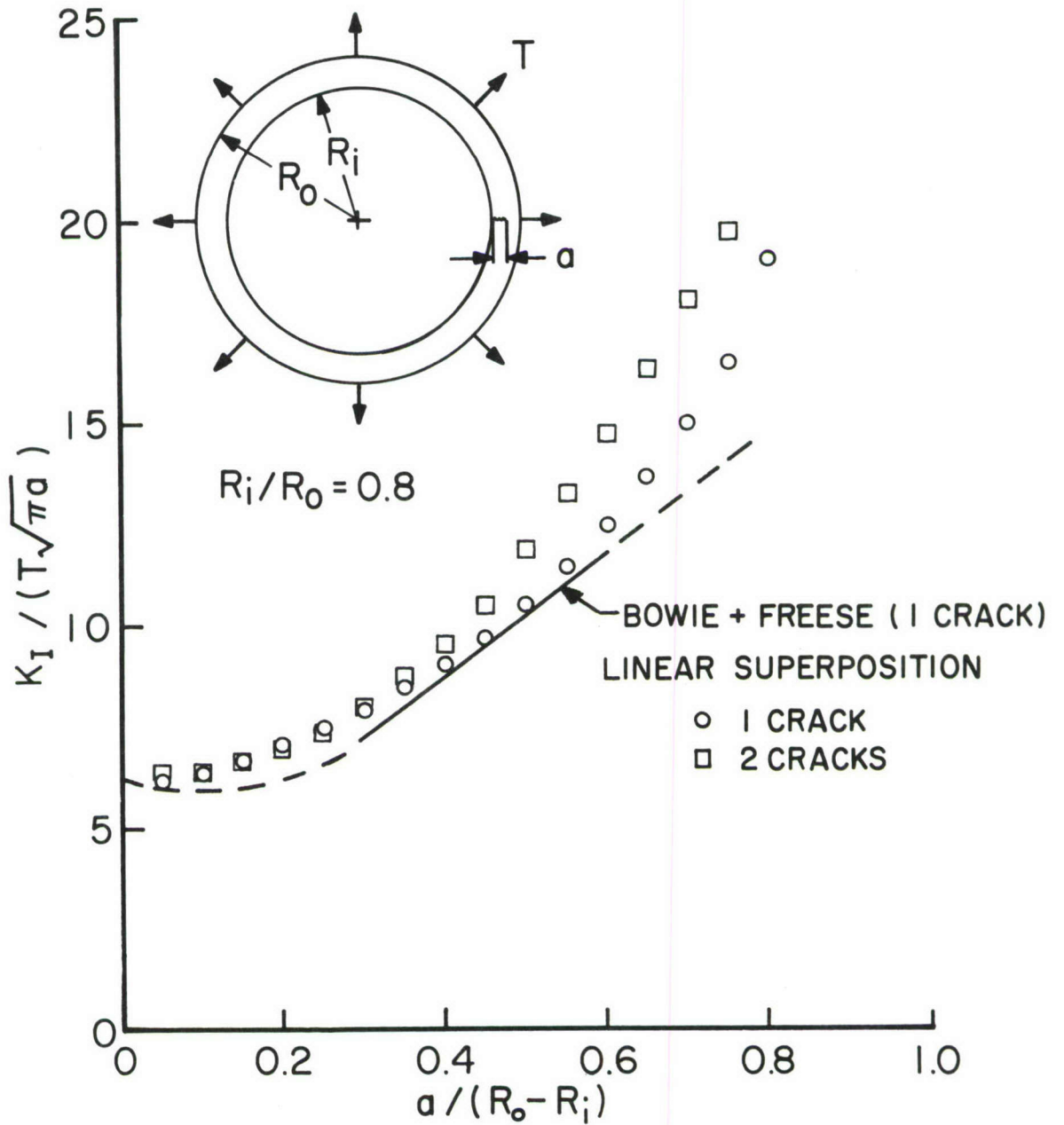


Figure 5. Stress Intensity Factor Calibration for a Cracked Ring Loaded in Remote Tension ( $R_i/R_o = 0.8$ )

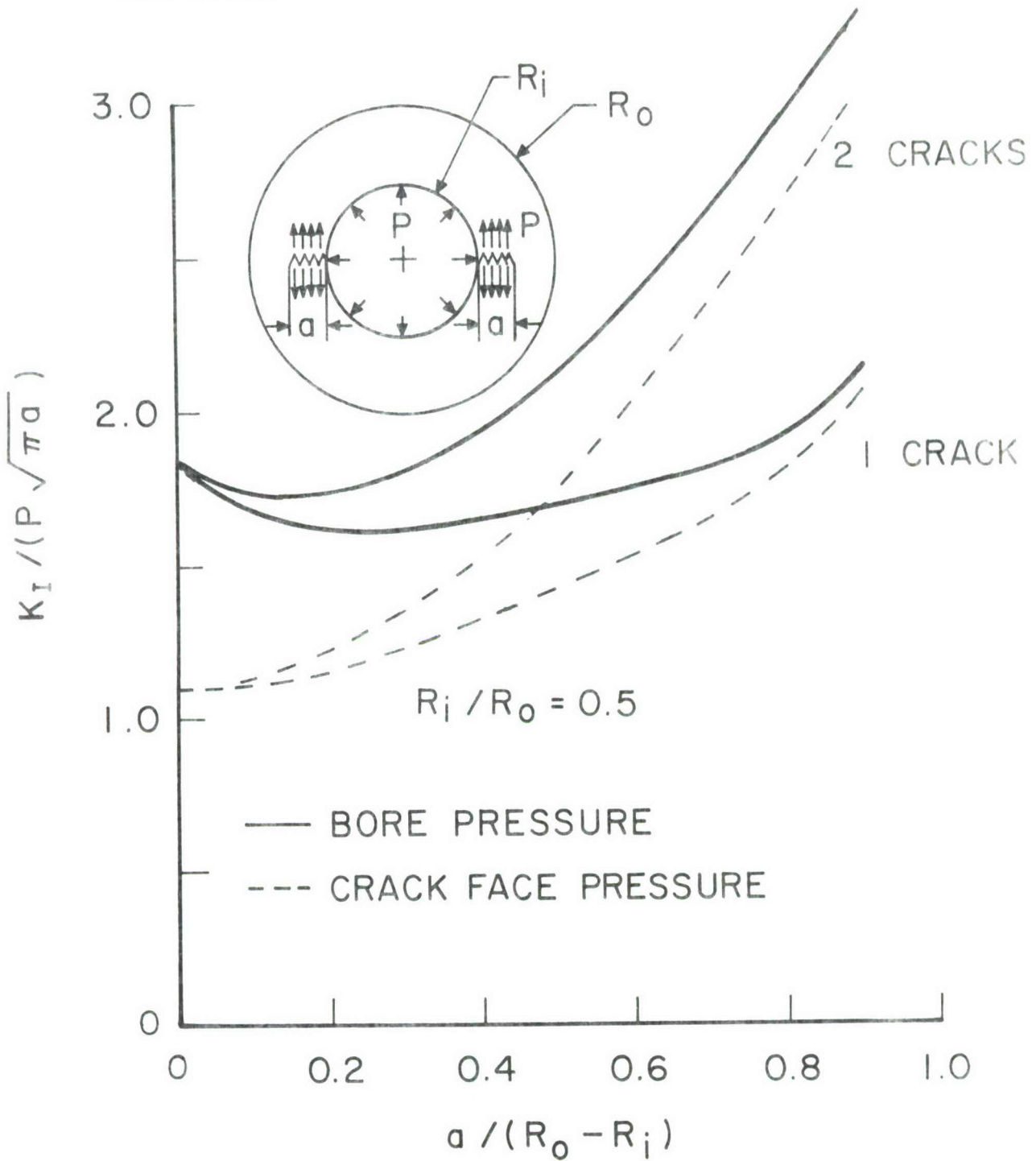


Figure 6. Stress Intensity Factor Calibration for a Cracked Cylinder Under Internal Pressure ( $R_i/R_o = 0.5$ )

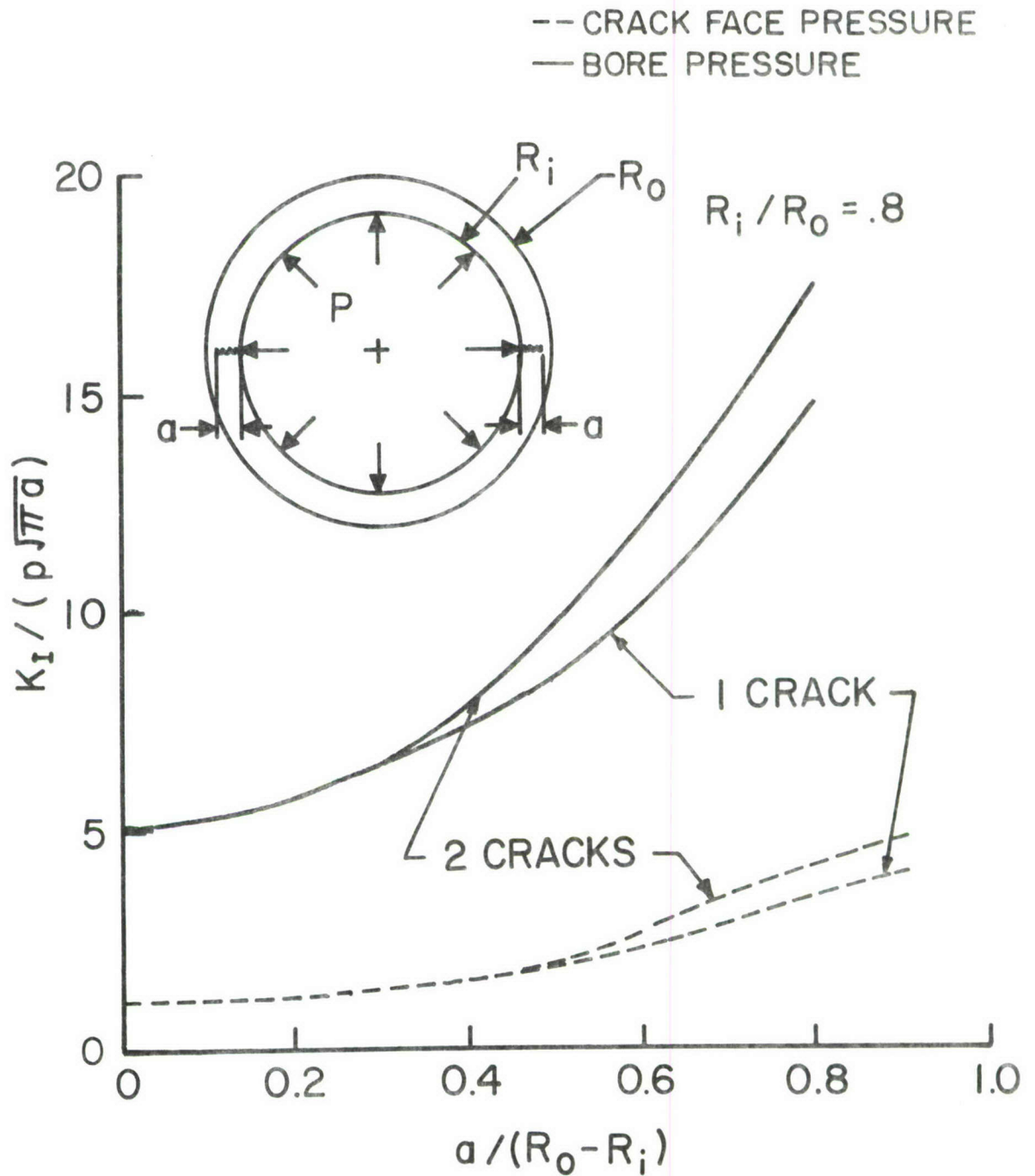


Figure 7. Stress Intensity Factor Calibration for a Cracked Cylinder Under Internal Pressure ( $R_i/R_0 = 0.8$ )

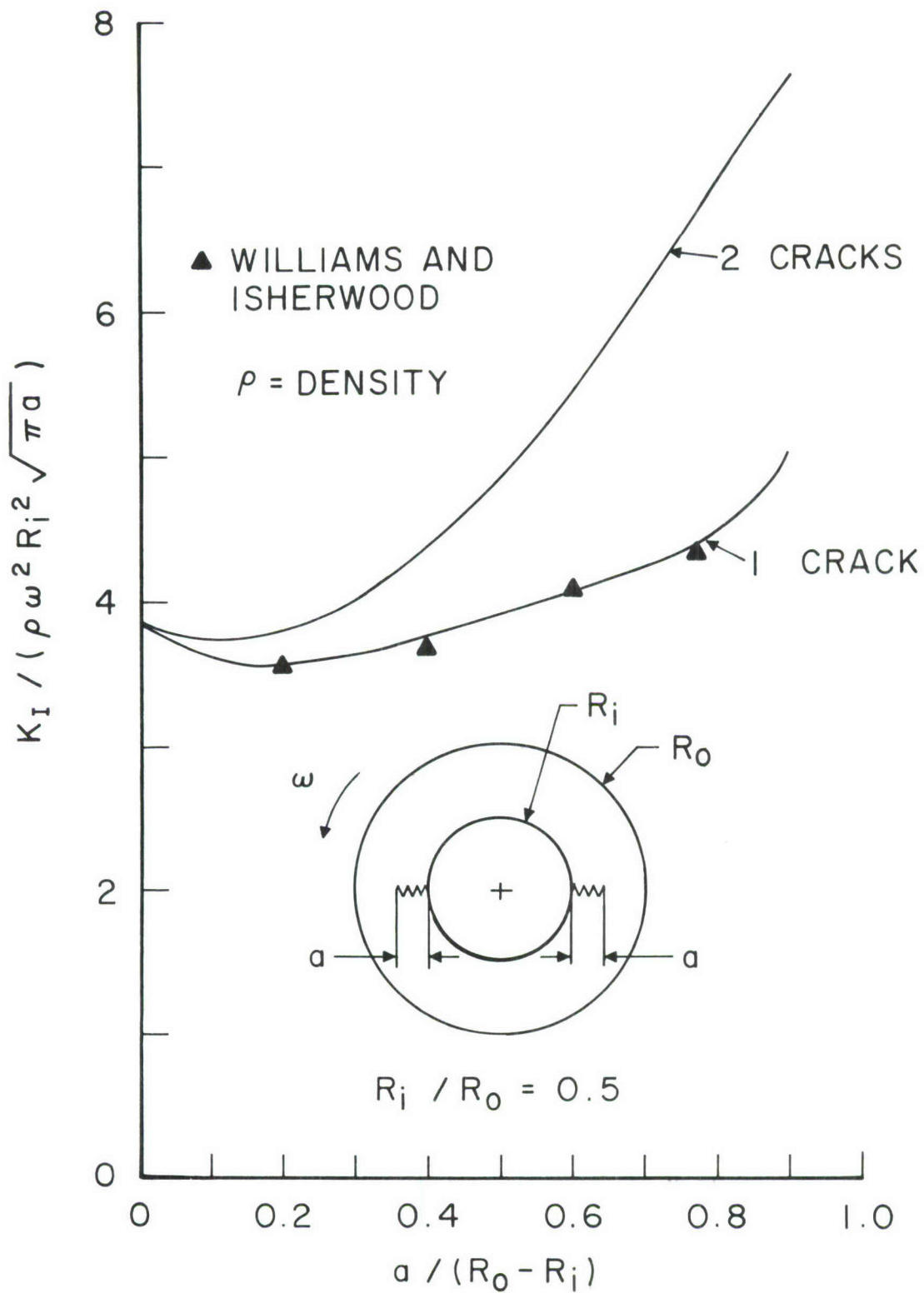


Figure 8. Stress Intensity Factor Calibration for a Cracked Ring Rotating With Angular Velocity  $\omega$



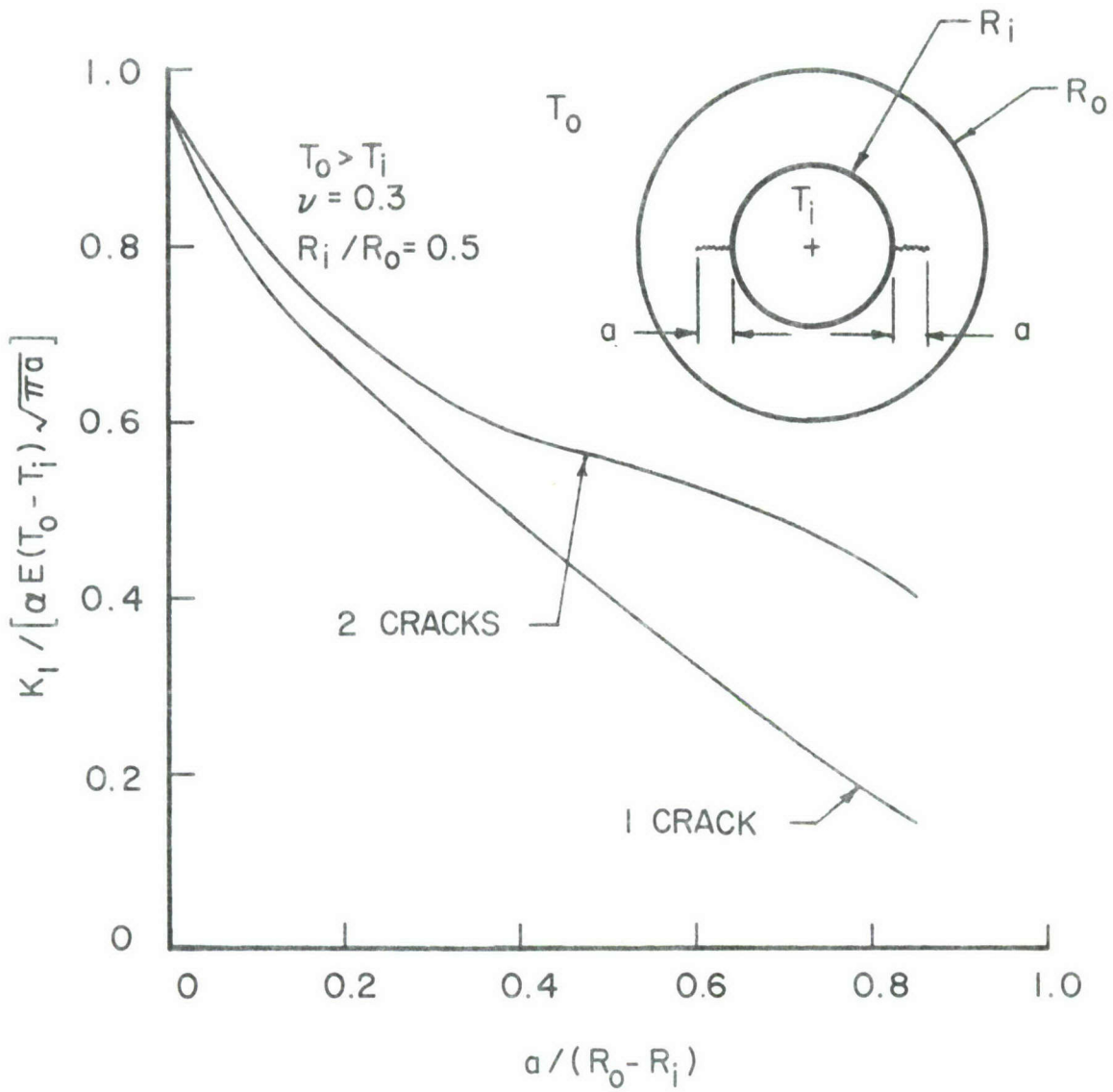


Figure 10. Stress Intensity Factor Calibration for a Cracked Ring Subjected to a Thermal Gradient.

## REFERENCES

1. A. F. Grandt, Jr., "Stress Intensity Factors for Some Thru-Cracked Fastener Holes," International Journal of Fracture, Vol. 11, No.2, 1975.
2. P. C. Paris, M. P. Gomez, and W. E. Anderson, "A Rational Analytical Theory of Fatigue," The Trend in Engineering, Vol. 13, No. 1, January 1961, University of Washington.
3. A. F. Emery, "Stress-Intensity Factors for Thermal Stresses in Thick Hollow Cylinders," Journal of Basic Engineering, Transactions of the ASME, Series D, Vol. 88, No. 1, March 1966, pp 45-53.
4. A. F. Emery, G. E. Walker, Jr., and J. A. Williams, "A Green's Function for the Stress Intensity Factors of Edge Cracks and Its Application to Thermal Stresses," Journal of Basic Engineering, Transactions of the ASME, Series D, Vol. 91, No. 4, December 1969, pp 618-624.
5. H. F. Bueckner, "Weight Functions for the Notched Bar," Zeitschrift fur Angewandte Mathematik and Mechanik, Vol. 51, 1971, pp 97-109.
6. O. L. Bowie, "Analysis of an Infinite Plate Containing Radial Cracks Originating from the Boundary of an Internal Circular Hole," Journal of Mathematics and Physics, Vol. 35, 1956, pp 60-71.
7. A. F. Grandt, Jr. and T. D. Hinnerichs, "Stress Intensity Factor Measurements for Flawed Fastener Holes," Proceedings of the Army Symposium on Solid Mechanics, 1974; The Role of Mechanics in Design-Structural Joints, AMMRC MC 74-8, Army Materials and Mechanics Research Center, Watertown, Mass., September 1974, pp 161-176.
8. J. R. Rice, "Some Remarks on Elastic Crack-Tip Stress Fields," International Journal of Solids and Structures, Vol. 8, No. 6, June 1972, pp 751-758.
9. R. Labbens, A. Pellissier-Tanon, and J. Heliot, "Practical Method for Calculating Stress-Intensity Factors Through Weight Functions," presented at the Eighth National Symposium on Fracture Mechanics, Brown University, Providence, R.I., August 1974.
10. A. T. Jones, "A Radially Cracked, Cylindrical Fracture Toughness Specimen," Engineering Fracture Mechanics, Vol. 6, No. 3, October 1974, pp 435-446.
11. T. W. Orange, "Crack Shapes and Stress Intensity Factors for Edge-Cracked Specimens," Stress Analysis and Growth of Cracks, Proceedings of the 1971 National Symposium on Fracture Mechanics, Part I, ASTM STP 513, American Society for Testing and Materials, 1972, pp 71-78.

12. S. Timoshenko and J. N. Goodier, Theory of Elasticity, McGraw-Hill, 1951.
13. O. L. Bowie and C. E. Freese, "Elastic Analysis for Radial Crack in a Circular Ring," Engineering Fracture Mechanics, Vol. 4, No. 2, June 1972, pp 315-321.
14. A. P. Boresi, "Elasticity in Engineering Mechanics," Prentice Hall, 1965.
15. J. G. Williams and D. P. Isherwood, Calculation of the Strain-Energy Release Rates of Cracked Plates by an Approximate Method," Journal of Strain Analysis, Vol. 3, No. 1, 1968, pp 17-22.
16. D. R. J. Owen and J. R. Griffiths, "Stress Intensity Factors for Cracks in a Plate Containing a Hole and in a Spinning Disk," International Journal of Fracture, Vol. 9, No. 4, December 1973, pp 471-476.
17. Data discussed during review of Air Force Contract Number F33615-73C-5109 with Southern Research Institute, entitled "Fracture Mechanics of Graphitic Materials", September 13, 1974.
18. Airplane Damage Tolerance Design Requirements, Military Specification MIL-A-83444 (USAF), May 1974.